Static and Dynamic FT-IR Linear Dichroism Studies of Plasticization Effects in a Polyurethane Elastomer

Darla K. Graff,[†] Haochuan Wang,[‡] Richard A. Palmer,*[,‡] and Jon R. Schoonover*[,†]

Chemical Science and Technology, CST-4, MS J586, Los Alamos National Laboratory, Los Alamos, New Mexico, 87545, and Department of Chemistry, Duke University, Durham, North Carolina 27708

Received April 5, 1999; Revised Manuscript Received August 3, 1999

ABSTRACT: By combining FTIR data of plasticized Estane (a polyester polyurethane copolymer) subjected to mechanical deformation with spectral differences as a function of added plasticizer, insight into the physical role of plasticization is gained. For Estane, the orientation functions and dichroic difference data show that, in static stretching, the soft domains reach orientation saturation before the hard domains. With added plasticizer, hydrogen bonding to the hard segments is disrupted and the glass transition of the soft domain decreases, indicating that plasticizer remains solubilized in the soft domain. On the time scale of the static experiment, plasticization diminishes the ability of both domains to reorient, while the plasticizer itself does not orient. With added plasticizer, neither domain reaches orientation saturation during the prestretching process, and dynamic distortion results in a similar response from both domains. Bimodal bands in the dynamic data indicate that the strain applied on a rapid time scale (20 Hz) allows resolution of the components of differently oriented bands.

Organic block copolymers represent a class of materials with variable properties and applications. Because of the direct relationship between microscopic structures and macroscopic properties, a number of different molecular spectroscopic techniques have been applied to the study of these systems.[1,2] Vibrational spectroscopy is a particularly insightful approach since the spectra are sensitive to molecular orientation, conformation, isomerization, and crystallinity. Advances in Fourier transform infrared (FT-IR) absorption methods have led to a number of important studies on polymer systems, including rapid-scan FT-IR rheo-optic techniques[3−7] and applications of dynamic step-scan FT-IR.[8−15]

Static dichroic FT-IR spectra collected at stepwise stretching intervals of a polymer provide direct information on molecular-level orientations which accompany the bulk stretch. These data can be directly compared to rheological measurements.[16] Similarly, recently developed dynamic dichroic FT-IR methods allow monitoring of vibrational dipole orientations when the system is subjected to a dynamic, oscillating tensile deformation.[9,14] As it is usually applied, this technique involves the combination of dynamic mechanical analysis (DMA) and time-resolved infrared spectroscopy to study real-time infrared spectral changes in polymer films under sinusoidal tensile stress of small amplitude. Phase-locked electronics are used to record the dynamic infrared spectral changes in-phase and in-quadrature with the applied mechanical field. The in-phase and in-quadrature signals correspond to responses that are perfectly elastic and viscous, respectively, at the given frequency of the oscillating mechanical field. These measured signals can be used to calculate the relative rates at which different functional groups and segments respond to the applied dynamic strain.

Estane is the name of a family of polyester polyurethane segmented block copolymers.[17−19] In such copolymers, the polyurethane segments associate with one another to form hard domains which act as pseudo-cross-links between polyester soft domains.[20] This morphology provides the distinctive thermal and mechanical properties of the material and accounts for its usefulness in a wide range of applications. The material of interest in this study is Estane 5703, which is a relatively soft polyester/polyurethane copolymer,[17] consisting of approximately 70% soft and 30% hard domains. Estane and similar copolymers have proven to be good candidates for study using static and dynamic dichroic FT-IR.[11,13] The soft and hard domains tend to respond differently to mechanical stress, and the molecular-level changes that accompany the large-scale deformations are easily observed.

In some of its applications, Estane 5703 is combined with a plasticizing compound in as high as a 50%/50%, by weight, mixture. The addition of this plasticizer has been observed to decrease the stress at break, increase the strain at break (to a point), and decrease the Young's modulus of the elastomer.[21] Our motivation is to use dichroic FT-IR methods to observe and quantify the molecular-level responses as Estane 5703 undergoes static and dynamic mechanical deformation and to compare these responses in samples containing increasing amounts of plasticizer. Plasticizer has been observed to decrease the glass transition of the elastomeric soft domain[26] and is anticipated to effect the hard and the soft domains differently.[22] A study of the effect of plasticization on polymer deformation properties can provide insight into the structural role played by the plasticizer in the polymer system.

Experimental Section

Estane 5703, poly(butylene adipate)−poly(4,4′-diphenylmethane diisocyanate−1,4-butanediol), was obtained in pellet form from B.F. Goodrich. The nitroplasticizer (NP) is a 50/50 wt % blend of bis(2,2-dinitropropyl)formal and bis(2,2-dinitropropyl)acetal.

A series of 16 NP/Estane composites were mixed with percentages of NP varying from 0 to 50 wt %. Solutions (2 wt % solids in methyl ethyl ketone, Fisher) were cast on BaF_2

[†] Los Alamos National Laboratory.
[‡] Duke University.
* Corresponding author.

10.1021/ma990495g CCC: $18.00
Published on Web 10/01/1999

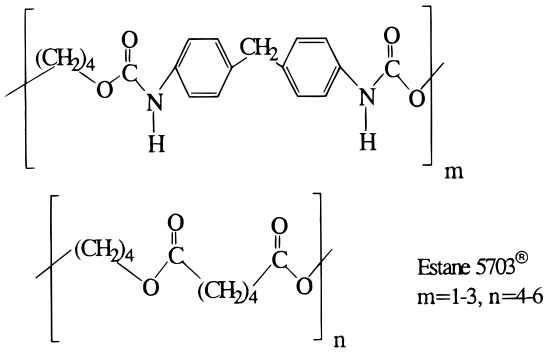

plates and dried in a conventional oven at 60 °C for 24 h for solvent removal.

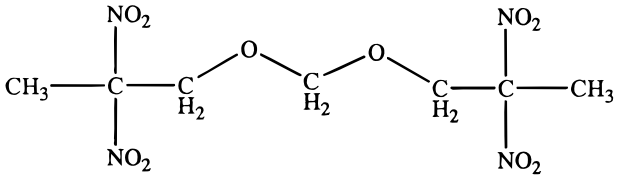

BDNPF, bis(2,2-dinitropropyl)formal

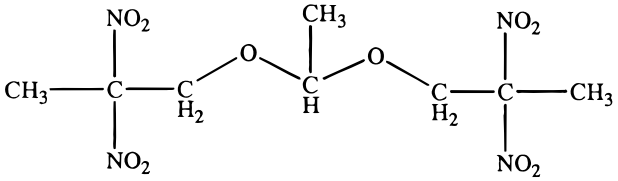

BDNPA, bis(2,2-dinitropropyl)acetal

Bulk FT-IR spectra were measured in the rapid scan mode using a Nicolet 20SXB equipped with a DTGS detector and sample shuttle system. For each spectrum, 128 scans were averaged at a spectral resolution of 4 cm^{-1} (800−3800 cm^{-1}). A multifile linear baseline routine was used (GRAMS, Galactic Industries Corp.) to obtain a least-squares linear baseline for each of the 16 spectra using the same 20 baseline points as the fitting criterion.

For the stretching experiments (both static and dynamic), thin films of 0, 10, 20, and 30 wt % of NP in Estane 5703 were solvent cast out of a 15 wt % solution of solids in methyl ethyl ketone. Casting solutions were spread on a Teflon sheet using a 7 μm knife blade, and the solvent was allowed to evaporate at room temperature for several hours before the films were dried in a conventional oven for 3 days at 60 °C.

The step-scan FT-IR instrument used in the static and dynamic stretching experiments is a Bruker Optics IFS66/DSP equipped with a mercury cadmium telluride (MCT) detector.[11] A low-pass optical filter (4000 cm^{-1} cutoff) was used, and data were measured with 4 cm^{-1} resolution. Static stretching experiments were conducted using the rapid-scan mode of this instrument and a wire-grid polarizer to alternate the light polarization between parallel and perpendicular at each stretching position. A polymer film, 0.5 cm in length, was clamped into the jaws of a stretcher with a 7 cm stretching capacity. The polymer was placed in the sample chamber with its stretching direction vertical, and each polymer sample was stretched in ca. 0.5 cm increments. A 15 min purge time was used between the stretching and the spectral measurements.

The static stretching data provide vibration-specific (functional group specific) dichroic information pertaining to the preorientation of the polymer sample prior to the dynamic measurement. One particularly useful means of evaluating static dichroic data is to calculate orientation functions for the various infrared intensity changes observed as a function of stretching distance.[5,7] The orientation function calculation removes the intensity contributions that arise from the various dipole strengths of the different vibrational modes of the polymer. This approach provides orientation parameters from each normal mode on a similar scale for direct comparison. The orientation function is calculated from dichroic spectra using the following expression:[7]

$$f = \frac{(R-1)(R_0+2)}{(R_0-1)(R+2)} = \frac{3\langle(\cos\theta)^2\rangle - 1}{2} \tag{1}$$

where R is the dichroic ratio of a given absorption band ($A_\parallel/A_\perp$), and $R_0 = 2 \cot 2\psi$ and is the dichroic ratio for perfect orientation. The angle ψ is between the polymer chain axis and the specific vibrational dipole, and the angle θ is between the polymer chain axis and the direction of the deformation. Assuming only vibrations with $\psi = 0°$ and $\psi = 90°$, the orientation function reduces to

$$f_\parallel = \frac{R-1}{R+2} \tag{2a}$$

and

$$f_\perp = -2\frac{R-1}{R+2} \tag{2b}$$

Static stretching data can also be analyzed with the orientation effects removed. The averaged dipole strengths and distributions of the polymer system are then viewed in an orientation-averaged manner.[7] The structural absorbance spectrum (A_0) is calculated from parallel and perpendicular static spectra at each point in the static stretch:

$$A_0 = \frac{A_\parallel + 2A_\perp}{3} \tag{3}$$

Static stretching data were measured on films of pure Estane, Estane with 10% nitroplasticizer (NP10), and Estane with 20% nitroplasticizer (NP20). Each film was stretched to its break point. Orientation functions were calculated for the majority of bands in the spectrum. Equations 2a and 2b were used, the value of ψ (0 or 90°) being chosen for each mode on the basis of the polymer structure and normal-mode composition. Additionally, structural absorbance spectra were calculated for the Estane, NP10, and NP20 spectra at 100% and 700% strain. A difference spectrum in each case was collected using the 100% strain spectrum as the subtrahend and a multiplicative factor that minimized the spectral difference in the 2700−3100 cm^{-1} spectral range. On the basis of the calculated thickness change (assuming constant volume with uniaxial stretch), the multiplicative factors used in the spectral subtraction were too large by 180% (Estane), 100% (NP10), and 40% (NP20). This discrepancy was likely due to slight "necking" as the films were stretched and indicates relatively large margins of error in the calculation of A_0 spectra.

The Bruker Optics IFS66/DSP was used for the dynamic measurements. A sinusoidal tensile strain at 20 Hz was applied to the polymer film by a Polymer Modulator (Manning Applied Technology). The details of the approach for conducting the dynamic stretching experiment have been published previously.[11] Briefly, a ZnSe photoelastic modulator (PEM) (ZnSe50, Hinds Instruments Inc.) is used to generate broadband polarization modulation in the mid-infrared region. The PEM modulation amplitude was set so that the first node in the output efficiency was at 1900 cm^{-1}, providing a high throughput of modulated light through the spectral regions of interest (1000−1800[1] and 2800−3500 cm^{-1}). The fundamental frequency of the PEM is 50 kHz, which produces alternating parallel and perpendicularly polarized infrared light at a frequency of 100 kHz. The stretcher is modulated at 20 Hz, and in theory, the light beam can additionally be modulated by the interferometer at 366 Hz. The signal in this case would be the result of a triple modulation. An alternate approach, which we used, is to decouple the step-scan inter-

ferometer by turning off the dithering of the mirror position. The dynamic experiment then involves only polarization and stretching modulations which are demodulated using two lock-in amplifiers.

To obtain a dynamic dichroic difference spectrum in infrared absorbance units, four different measurements are made. Two measurements correspond to the ac component of the dynamic signal and two to the dc component. The first two measurements are referred to as "second polarizer measurements" and result in transmission spectra I_{max} and ΔI_{max}. These measurements are performed with the sample removed from the path of the beam. For the first spectrum, a second polarizer is inserted to provide a maximal anisotropy signal. With the PEM turned on, the signal is demodulated at 100 kHz and directed through a low-pass filter. This measures the transmission spectrum ΔI_{max} and provides the Fourier transform phase which is used to phase-correct the subsequent ΔI and $\Delta\Delta I$ sample measurements. With the second polarizer still in place, the second measurement is performed. The retardation modulation of the interferometer is turned on, and a low-pass filter removes the polarization modulation from the signal. The signal is demodulated by the digital signal processor (DSP) of the infrared bench and results in the I_{max} transmission spectrum. The second polarizer is then replaced by the sample, and the previous measurement repeated, resulting in the I_{sample} transmission spectrum. The sample is replaced by a chopper on the edge of the stretcher, positioned halfway into the beam. The mirror position of the interferometer is placed near the center burst, and the 20 Hz modulated signal is used to set the zero phase of the polymer stretcher on the lock-in amplifier. Once this is accomplished, the setting must stay fixed for the final measurement. The first of the "second polarizer" measurements is repeated, but with the sample in place of the polarizer. The doubly modulated signal crosses a high-pass filter where the 100 kHz component is demodulated by the first lock-in amplifier; the signal is then split, with the first crossing a low-pass filter and resulting in a static dichroic difference transmission spectrum, ΔI_{static}. The second part of the signal is demodulated at 20 Hz by the dual-channel lock-in amplifier which outputs an in-phase and an in-quadrature dynamic dichroic difference transmission spectrum, $\Delta\Delta I_{in-phase}$ and $\Delta\Delta I_{in-quad}$, respectively. The four measurements result in six total transmission spectra: ΔI_{max}, I_{max}, I_{sample}, ΔI_{static}, $\Delta\Delta I_{in-phase}$, $\Delta\Delta I_{in-quad}$. The first three spectra are used to convert the latter three spectra from transmittance to absorbance, using the following equation:

$$\Delta A_{corr} = -\left(\frac{\Delta\Delta I^*_{sample}}{I_{sample}}\right)\left(\frac{I_{max}}{\Delta I_{max}}\right) \quad (4)$$

where ΔA_{corr} indicates the corrected, normalized dichroic difference absorption spectrum, and $\Delta\Delta I_{sample}$ represents any one of the three dynamic transmittance spectra (ΔI_{static}, $\Delta\Delta I_{in-phase}$, or $\Delta\Delta I_{in-quad}$). The symbol * is used to indicate that the Fourier transform of this interferogram was recalculated using a Mertz phase-correction algorithm and the phase obtained from the ΔI_{max} spectrum.

Dynamic measurements were performed on polymer films of Estane, Estane with 10% nitroplasticizer (NP10), Estane with 20% nitroplasticizer (NP20), and Estane with 30% nitroplasticizer (NP30). All films were prestretched to approximately 600% their original length.

For normalization of the static spectra, regular FT-IR absorption spectra of the unstretched polymer films were taken of a solvent-cast sample on 13 × 2 mm BaF_2 windows after drying 24 h at 60 °C in a conventional oven. Additionally, for reference, a spectrum of the viscous nitroplasticizer liquid was measured on a KBr pellet. These spectra were measured on the Nicolet 20SXB FT-IR bench.

Results

In Figure 1 are shown regular FT-IR absorption spectra of pure Estane and pure NP (800−3500 cm^{-1}).

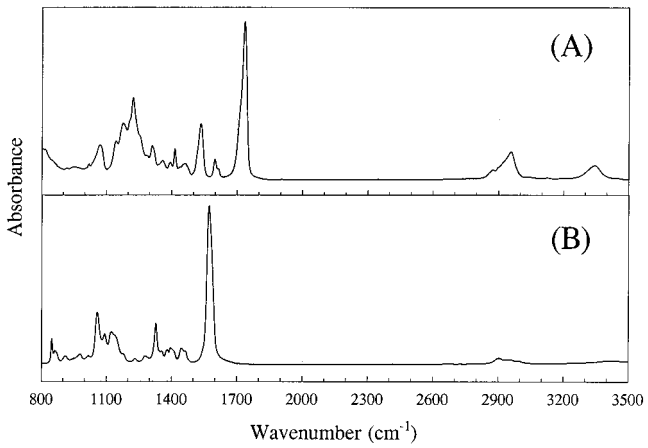

Figure 1. FT-IR absorption spectra of (A) pure Estane, solvent cast film, and (B) pure nitroplasticizer, KBr pellet. The major bands with normal-mode assignments are listed in Table 1.

Table 1. Band Assignments (1050−3500 cm^{-1}) for Polyester Polyurethane, Estane 5703, and Nitroplasticizer

freq (cm^{-1})	rel int	assignment	domain origin
1074	strong	ν(C−O−C) urethane and ester	hard and soft
1143	weak		
1174	strong	ν(C−O−C) ester	soft
1223	strong	ν(C−N) + δ(N−H)	hard
1252	strong	ν(C−O−C) ester; w(CH_2)	soft
1311	weak	ν(C−N) + δ(N−H); phenyl ring 3 (primarily	hard
1362	weak	w(CH_2)	soft
1394	weak	w(CH_2)	soft
1415	weak	phenyl ring 19b (primarily ν(C−C))	hard
1464	weak	δ(CH_2)	soft
1533	strong	ν(C−N) + δ(N−H)	hard
1597	strong	phenyl ring 8a (primarily ν(C═C))	hard
1610	weak	phenyl ring 8b (primarily ν(C═C))	hard
1732	very	ν(C═O) urethane and ester	hard and soft
2870−3037	strong	ν(C−H)	hard and soft
3190−3440	strong	ν(N−H)	hard
1057	weak	ν_a(C−O−C−O−C)	NP
1093	weak	ν_s(C−O−C−O−C)	NP
1124	weak	ν_a(C−O−C−O−C)	NP
1328	weak	ν_s(NO_2)	NP
1572	very	ν_a(NO_2)	NP

The major vibrational bands with normal mode assignments are listed in Table 1. The bands are attributed to a domain origin in the polymer (hard segment, soft segment) or as NP for the nitroplasticizer.

Figure 2 shows difference spectra calculated using the 16 different NP/Estane composites ranging from 3 to 50% NP with NP = 0% as the subtrahend. Multiplicative factors were allowed to vary in the subtraction to account for variations in sample thickness. Subtractions were performed to minimize spectral differences.

Orientation functions calculated for several of the IR bands from the Estane, NP10, and NP20 static stretching spectra are plotted in Figure 3 versus percent strain. The vibrational bands with $\psi = 90°$ or 0° are indicated in parentheses. The bands at 1358, 1252, 1174, and 1143 cm^{-1} showed appreciable dichroic frequency shifts with increased stretching; for these bands, intensities were measured from the maxima (which shifted) as the polymer was stretched. The frequency positions of the

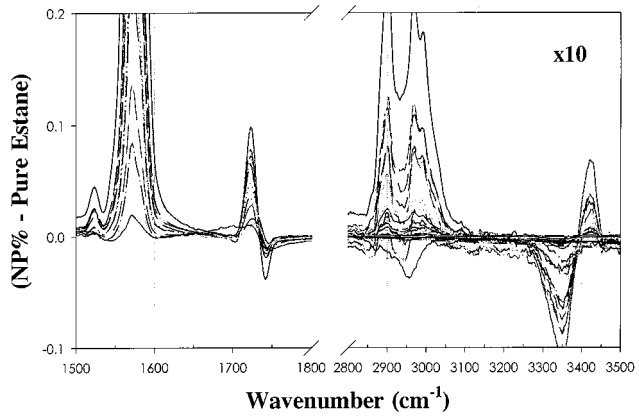

Figure 2. Difference spectra of 15 Estane composites with varying weight percent of NP, from 3% to 50%, with NP = 0% (pure Estane) as the subtrahend.

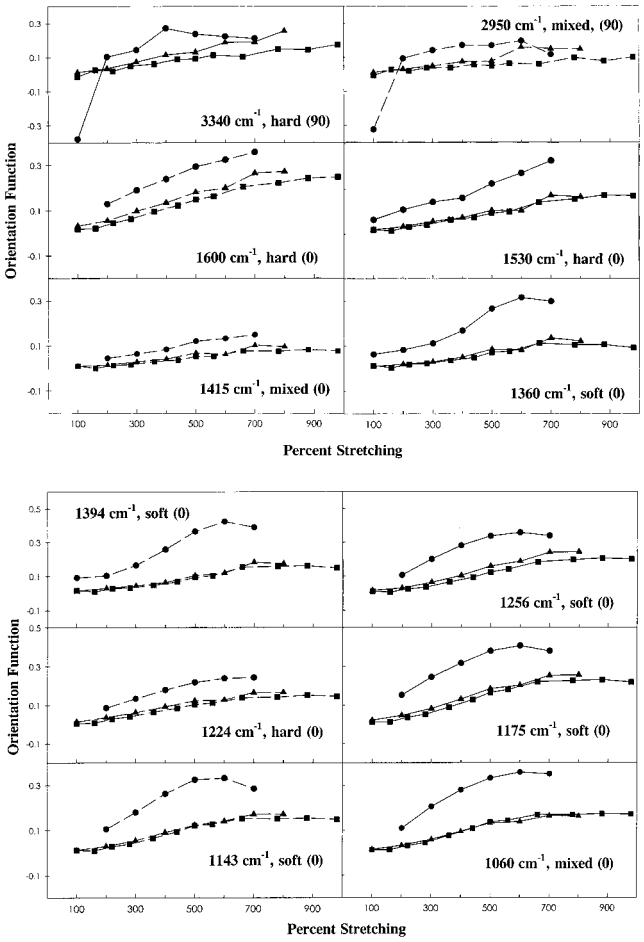

Figure 3. Orientation functions plotted versus percent stretching for Estane (●), NP10 (▲), and NP20 (■) solvent cast films. In each frame is listed the frequency, the domain origin of the band, and the value of ψ used in the calculation (0 or 90°).

parallel and perpendicular maxima for these four bands in Estane, NP10, and NP20 are plotted versus percent stretching in Figure 4. The band at 1143 cm^{-1} is a shoulder on the band at 1174 cm^{-1} with an identifiable maximum, but as it shifts to higher frequency, its maximum absorption can only be estimated.

In Figure 5, structural absorbance spectra, A_0, are presented for Estane, NP10, and NP20 at 100% and 700% strain. Difference spectra, calculated with the 100% strain spectrum as the subtrahend, are also

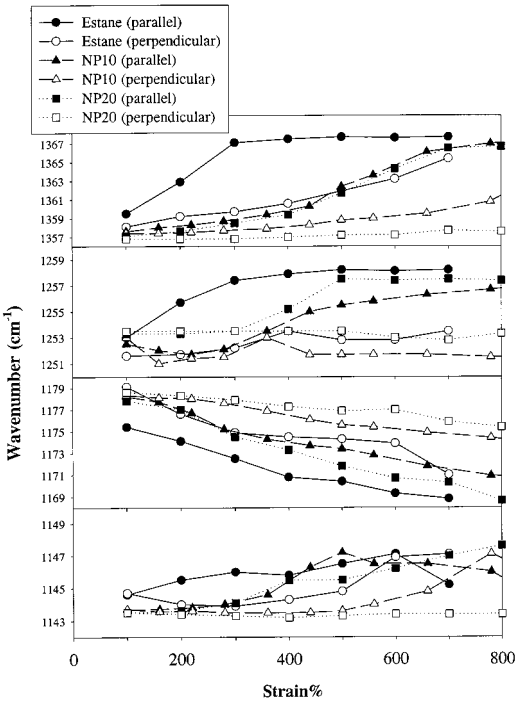

Figure 4. Parallel (filled) and perpendicular (hollow) frequencies plotted versus strain percent for Estane (●), NP10 (▲), and NP20 (■) films.

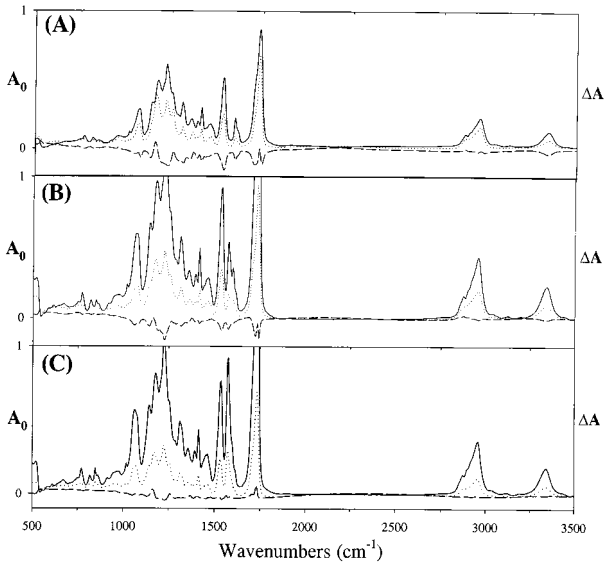

Figure 5. Structural aborbance spectra for (A) Estane, (B) NP10, and (C) NP20 at 100% and 700% static stretch (solid and dotted line, respectively). Difference spectra (dashed line) are shown, with subtraction minimizing differences in the 2700−3100 cm^{-1} region.

shown. The ν(C−H) region has been used in previous studies[4,7] as a reference band to account for thinning effects, so the subtraction was performed to minimize differences in this region (2700−3100 cm^{-1}).

The static spectra from the dynamic experiments are shown in Figure 6 for Estane, NP10, and NP20. These spectra are measured at the zero-crossing points of the sinusoidal stretch and therefore represent an average of the stretching perturbation. These spectra correspond to dichroic spectra measured when the polymer is stretched and held static. Each static spectrum is overlayed with its corresponding unstretched, regular

Table 2. "Normalized" (to 1256 cm^{-1} Band) Ratios of Static and Dynamic IR Bands

	ESTANE		NP10		NP20		NP30	
freq, cm^{-1}	stat/abs	dyn/stat	stat/abs	dyn/stat	stat/abs	dyn/stat	stat/abs	dyn/stat
1070.0 (m)	0.55	0.97	0.67	0.84	0.59	0.74	0.56	0.68
1147.0 (s)	0.70	1.90	0.55	1.00	0.51	0.66	0.55	0.80
1174.0 (s)	1.07	1.16	0.93	0.92	0.98	0.95	1.01	0.95
1225.0 (h)	0.59	1.95	0.41	0.69	0.45	0.68	0.54	0.61
1260.0 (s)	1.00	1.00	1.00	1.00	1.00	1.00	1.00	1.00
1309.0 (h)	0.64	1.51	0.59	0.51	0.60	0.35	0.65	0.31
1370.0 (s)	0.94	1.16	1.21	1.00	0.91	1.02	0.77	1.06
1395.0 (s)	0.73	1.01	0.79	0.55	0.54	0.64	0.49	0.59
1414.0 (m)	0.44	0.78	0.38	0.43	0.36	0.40	0.005	0.31
1460.0 (s)	−0.25	0.00	−0.09	0.00	−0.12	1.97	−0.06	3.62
1532.0 (h)	0.96	1.20	0.83	0.72	0.95	0.73	1.09	0.67
1596.0 (h)	0.67	0.99	0.59	0.86	0.52	0.73	0.53	0.66
1730.0 (m)	−0.40	2.75	−0.23	1.93	−0.23	2.36	−0.27	2.29
1570.0 (np)			0.01	0.00	−0.01	0.00	−0.02	1.00

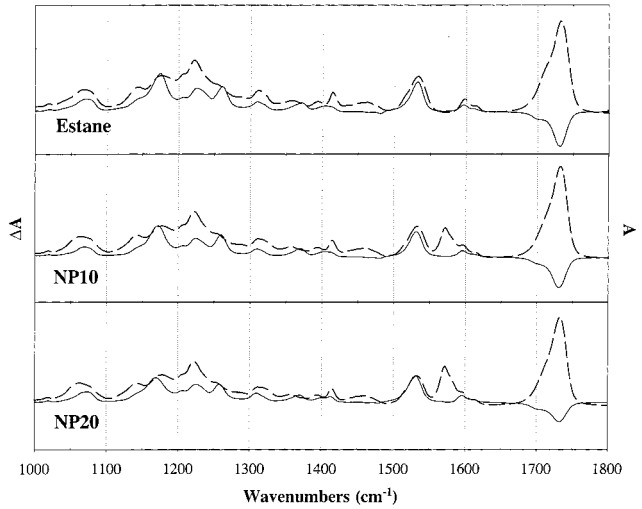

Figure 6. Static dichroic difference spectra (solid line) overlayed with FT-IR absorption spectra (dashed line). The spectra have been normalized such that the intensities of the 1252 cm^{-1} band are equal for comparison.

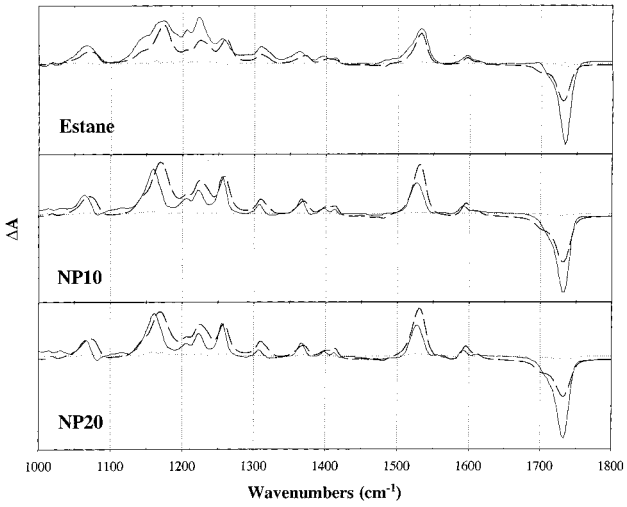

Figure 7. Dynamic dichroic difference spectra (in-phase and in-quadrature, solid and dotted lines, respectively) overlayed with the static dichroic difference spectra (dashed line), normalized such that the intensities of the 1252 cm^{-1} band are equal.

FT-IR absorption spectrum and normalized to give equal intensity for the 1252 cm^{-1} band. The normalized ratios of the static to unpolarized band intensities (stat/abs) are given for these samples and NP30 in Table 2.

The in-phase and in-quadrature dynamic difference spectra for Estane, NP10, and NP20 are shown in Figure 7 along with an overlay of static difference spectra. The in-quadrature spectrum is extremely weak with intensity in the limit of experimental noise. This observation indicates that most of the polymeric response to the stretching perturbation at room temperature is elastic. The 1252 cm^{-1} band of each in-phase spectrum has been normalized to give equal intensity for this band in the corresponding static spectrum for comparison. Ratios of the normalized in-phase, dynamic-to-static band intensities (dyn/stat) are given in Table 2 for Estane, NP10, NP20, and NP30.

Discussion

FT-IR Studies. Plasticizers are compounds of low molecular weight added to polymeric materials to achieve desired physical properties. The effect of plasticization on the viscoelastic properties of a polymer depends on the specific plasticizer−polymer interactions and the amount and distribution of the plasticizer.[23] Because the plasticizer is effectively a soluble diluent of the polymer, it can affect the two domains of a block copolymer differently, depending on specific interactions and relative solubility.[22]

The role of hydrogen bonding in the formation of morphological structure in pure Estane is complex and not fully understood. However, thermal FT-IR studies performed on Estane,[24] and related systems,[25] indicate that marked spectral changes are indicative of changes in the hydrogen-bonding network of the soft and hard polymer domains. These thermal studies indicate hydrogen-bound and free components for the IR bands whose normal modes are involved in hydrogen bonding.

Estane 5703 has been studied as a function of nitroplasticizer concentration using FT-IR, thermal FT-IR, and differential scanning calorimetry (DSC).[26] In these data, the effect of NP on the morphology is manifested by the hydrogen-bonding changes as a function of the concentration of NP. The room-temperature FT-IR difference spectra of 15 Estane films with by weight percentages of added NP ranging from 3% to 50% (Figure 2) show distinct changes in the hydrogen-bonding pattern of urethane hard segments. The relative change in hard versus soft segments is obscured by the presence of NP bands which mask most of the relevant soft-segment bands. However, the addition of NP clearly causes a decrease in the hydrogen bonding associated with the urethane segments, with the intensity of the hydrogen-bound ν(N−H) component at 3340

cm^{-1} decreasing and the free component at 3420 cm^{-1} increasing. This decrease in hydrogen bonding is also evident in the δ(N−H) + ν(C−N) band, with the free component at 1520 cm^{-1} gaining intensity. The concomitant decrease in intensity of the hydrogen-bound component at 1540 cm^{-1} is masked by the growing intensity of the NP band at 1570 cm^{-1}.

The ν(C═O) region shows distinct changes as well; however, this region is complicated by having significant contributions from both the hard and soft segments. For both segments, the hydrogen-bound and free components are observed to occur at 1704 and 1732 cm^{-1}, respectively. The difference spectra indicate a large growth of the free component which is shifting to lower wavenumber with increasing NP content. This shifting band nearly conceals a small decrease which is observable in the hydrogen-bound component near 1705 cm^{-1}. One interpretation consistent with the observed spectral changes in this region and those previously mentioned is that the NP is disrupting hydrogen bonding in the hard segments, so that the bound component is decreasing. As the phase separation of domains in Estane is not complete, it is not clear whether these hydrogen-bonding changes arise predominantly from the hard segments that remain dissolved in the soft domain, the hard-segment aggregates that form the hard domain, or the hard segments at the interface of the two domains. In this interpretation, the soft segments, containing by far the larger proportion of free ν(C−O) groups, are then responsible for the downward shift in vibrational frequency of the 1732 cm^{-1} band with increasing NP content. This interpretation is well-supported by spectra obtained from adding NP to poly(butyl adipate), a model compound of the soft segment (data not shown). In this experiment, addition of NP was seen to shift the 1732 cm^{-1} band almost identically to the shift observed for Estane. The observations are consistent with a solubilizing effect of NP on the soft segments. Differential scanning calorimetry (DSC) results for samples containing varying amounts of NP indicate a 3 °C decrease in the soft-segment glass transition for every 10% increase in NP concentration. This decrease in the soft-segment T_g supports the idea that a large percentage of the NP remains solubilized in the soft domain. The FT-IR difference spectra and DSC results suggest that the largest effects of NP addition are the decrease in hydrogen bonding of the hard segments and solublization of the soft segments.

Static FT-IR Linear Dichroism Studies. The polarized spectra from the static stretching experiments indicate that the polymer backbone aligns in the stretching direction as stretching is increased. In dichroic difference spectra, bands from vibrational dipoles that are parallel to the polymer chain axis appear with positive intensity, while those that are perpendicular to that axis (ν(C−H), ν(C═O), ν(N−H)) are negative. The NP bands, which have considerable intensity in unstretched regular FT-IR spectra, have little or no intensity in the dichroic difference spectra. This observation indicates that the NP dipoles are only very weakly oriented upon stretching. Only the most intense NP band (1570 cm^{-1}) demonstrates enough intensity to be analyzed, and its orientation functions were extremely small (near zero) for all samples at all degrees of stretching.

By expressing polarized static stretching information as orientation functions, all vibrational bands are viewed on an equivalent scale where intensity indicates degree of orientation independent of individual dipole strengths. The orientation functions for 12 bands from the pure Estane sample are plotted in Figure 3. The ν(N−H) and ν(C−H) bands have inherently low intensities and are the most effected by baseline effects in the stretching data. The bands with the highest orientation functions are associated with the soft segment of the polymer. (The scales of the various plots are not equal.) Additionally, the orientation functions assignable to the soft segments have functional forms that are notably different from those arising from the hard. The soft-segment functions are more sigmoidal in shape, reaching their maximal value by ca. 600% stretch. Hard-segment functions are more linear and are still increasing at the time of polymer break. The orientation function magnitude for a perfectly oriented sample is 1.0; however, Siesler et al.[5] have calculated that, on the basis of the urethane crystal structure, the highest orientation function to be expected is 0.65. Our values approach this limit.

For every IR band plotted in Figure 3, comparison of orientation functions for samples with increasing NP concentration indicates that the presence of NP, even at only 10%, drastically decreases the ability of the polymer to orient or to remain oriented on the 15 min time scale of the static experiment. For the 1530 and 1256 cm^{-1} bands, the effect of increasing NP concentration is monotonic (i.e., the orientation functions continue to show a further decrease on going from NP10 to NP20, although the effect is very weak). In most of the bands, the increase of NP content from 10% to 20% does not result in a significant further decrease. In the NP10 and NP20 data, the functional forms of hard and soft behaviors are not as distinguishable as they are in the case of pure Estane. The presence of the plasticizer has an equalizing effect on the two domains in terms of their orientational response to static stretching.

In addition to orientation effects, the polarization spectra of statically stretched samples (Figure 4) show distinct frequency differences for four bands: 1358, 1252, 1174, and 1143 cm^{-1}. These bands are all assigned to vibrations associated with the soft segment. This observation is consistent with the conclusions drawn from the orientation functions, that is, that the soft segments display the effects of stress more strongly than the hard. The observed frequency shifts are due to the different ways in which lengthwise stress changes the various normal mode compositions. Infrared and Raman frequency shifts have been observed in static stretching experiments conducted on other polymers.[27−31]

The 1358 cm^{-1} band is largely comprised of the wagging motion of CH_2 groups. As the pure Estane sample is stretched, the parallel component of this band increases rapidly in frequency, shifting approximately 10 cm^{-1} within 300% strain. The perpendicular component increases by about 8 cm^{-1}, but with an onset of change delayed relative to the parallel (Figure 4A). The wagging motion of this normal mode involves a distortion of the angle between the H−C−H plane and the plane which bisects the C−C−C angle (same center carbons). As these chains are pulled parallel to the strain direction, the increased distortion of the soft-segment backbone (C−C−C angle) has a significant effect on the w(CH_2) vibrational frequency. At higher strains, the chains held perpendicular by the polymer

network begin to experience the bond angle distortion and a corresponding frequency shift. With the addition of 10% and 20% NP, the onset of the frequency shift for the parallel component is delayed by approximately 300% strain. Additionally, the perpendicular component of this band shifts less with increasing NP content. This observation is consistent with the orientation function results and demonstrates the molecular-level effect of the plasticization. The plasticizer compensates for this mechanical stress and delays the onset of stress in the polymer. As the static spectrum is collected 15 min after the sample is stretched, the data can also be interpreted as indicating a decrease in orientation relaxation time due to plasticization.

In Figure 4B, the parallel component of the 1252 cm^{-1} band shows a positive frequency shift of ca. 4 cm^{-1} from 100% to 700% stretch, while the perpendicular component shifts up 1−2 cm^{-1}. This band has contributions from both w(CH_2) and ν(C−O−C) of the soft segments. The w(CH_2) component has been discussed with respect to the 1358 cm^{-1} band. For the latter component, the C−O−C bond angle should also be very sensitive to backbone strain and distortion. The onset of the frequency shift in the perpendicular component is at a strain of ca. 400%, similar to the perpendicular component of the 1358 cm^{-1} band. With increasing NP%, the onset of the frequency shift is delayed in the parallel component by nearly 200% strain. The perpendicular components, in the presence of NP, do not show a significant frequency shift.

The 1174 cm^{-1} band is assigned to the asymmetric stretch of the ester C−O−C bond (ν_a(C−O−C)), and the 1143 cm^{-1} band is tentatively assigned to the symmetric C−O−C stretch. In the pure Estane sample, both the parallel and perpendicular components of these two bands shift significantly but in opposite directions with respect to each other. The 1143 cm^{-1} band is a shoulder on the more intense 1174 cm^{-1} band, causing some uncertainty in its frequency shift. The asymmetric ν-(C−O−C) band shifts to lower frequency with increased stress on the C−O bonds and C−O−C angle, while the symmetric ν(C−O−C) moves to higher frequencies. For both of these bands, the effect of increased NP is to diminish and delay the onset of the frequency shift.

In previous studies of other polymers subjected to uniaxial tensile stress,[27−29,31,32] two types of IR and Raman bands have been observed to display frequency shifts. The first type includes those bands with a large component of w(CH_2), and the second type involves bands that arise from backbone modes of the polymer and contain a large component of ν(C−C) stretch. In most cases, shifts were to lower frequency, consistent with an anharmonic theoretical treatment of the backbone ν(C−C) stretching vibrations.[30,31] For Estane, the ν(C−C) bands of the spectra are weak in intensity and largely masked by other bands. The frequency shifts that are observed arise from w(CH_2) and ν(C−O−C) bands, and three of the four bands shift to higher frequencies, not lower. Comparing frequency-shift behaviors of the different soft-segment modes in Figure 4, the bands containing significant w(CH_2) contributions appear to behave similarly, but quite differently from the bands that are predominantly ν(C−O−C). The w(CH_2) bands respond to the stress earlier. The parallel components of these bands also give rise to frequency shifts that are markedly different from the perpendicular. The ν(C−O−C) bands appear, in contrast, more stiff and constrained in a three-dimensional network with their frequencies being distorted with much less regard to orientation. The ν(C−O−C) functionality can engage in hydrogen bonding and electrostatic associations which will effect its vibrations and ability to orient, whereas the w(CH_2) component does not.

In the structural absorbance difference spectrum for pure Estane (Figure 5A), all the orientational contributions are removed to reveal the change in the average distribution of dipoles as the polymer is stretched.[16] The difference spectrum shows no indication of stress-induced crystallization (i.e., no new bands appear upon stretching). However, most of the positive features correspond to soft-segment bands (1732, 1370, 1260, and 1168 cm^{-1}), while the negative features (1598, 1534, 1415, 1313, and 1223 cm^{-1}) arise from the hard-segment bands. The frequency positions of the soft-segment bands (1168, 1260, and 1370 cm^{-1}) match well with the high strain values of the three most intense bands in Figure 4. The structural absorbance spectrum indicates specific conformations which are removed from or added to the system upon stretching. Thus, there is a slight increase in those soft-segment conformations that pertain to the strained state (from Figure 4). The ν(C═O) band at 1732 cm^{-1} shows a slight decrease in bandwidth upon stretching, consistent with fewer conformations in the stretched state. Addition of NP (Figure 5B,C) shows the same general pattern, but with diminished intensity of both positive and negative components with increasing NP.

Dynamic FT-IR Linear Dichroism Studies. Static dichroic difference data obtained from the dynamic experiment confirm many of the observations made from the statically stretched sample. Comparison of the static dichroic spectrum with the regular FT-IR spectrum of pure Estane demonstrates that the hard-segment bands (1060, 1223, 1311, 1415, 1534, 1598, and 1610 cm^{-1}) have lower intensity in the statically stretched spectrum. As with the orientation function plots of Figure 3, this observation demonstrates that at ca. 600% strain, the hard segments are less oriented than the soft and have not reached a point of orientation saturation. Two negative features in this region of the dichroic spectrum arise from bands whose vibrational dipoles are perpendicular to the polymer backbone (ν(C═O) at 1732 cm^{-1} and, less significantly, δ(CH_2) at 1462 cm^{-1}). In the higher wavenumber region (data not shown), the ν(N−H) and ν(C−H) bands also appear as negative features. The frequency shifts corresponding to the parallel components of the four soft-segment modes in Figure 4 are also observed in this data set. In addition, the 1394 cm^{-1} band shifts to higher frequency and begins to overlap with the 1415 cm^{-1} band, indicating significant changes in the δ(CH_2) modes sensitive to backbone orientation. The dichroic IR bands for the NP are very low in intensity or absent in the statically stretched samples, indicating that these small molecules remain randomly oriented upon tensile deformation.

The in-phase dynamic dichroic difference spectra (Figure 7) are normalized to the 1256 cm^{-1} band in the corresponding static dichroic difference spectrum. The in-quadrature dynamic dichroic difference spectra (multiplied by the same normalization factor as the in-phase component) are also overlaid. In all three samples, Estane, NP10, and NP20, the in-quadrature spectra are effectively zero, indicating that the dynamic response of the polymer is in-phase with the 20 Hz oscillating

stretch, i.e., is almost purely elastic. For the pure Estane sample, the hard-segment bands are significantly more intense in the in-phase dynamic dichroic spectrum than in the static dichroic spectrum. From the orientation functions at 600% strain (where the dynamic experiment was conducted), the soft-segment bands have reached orientation saturation (i.e., they demonstrate no additional orientation with strain), while the hard segments are still orienting linearly with strain. In other words, from this prestretched state, dynamic stretching has the largest effect on the hard-segment bands since they possess the ability to be oriented further.

In Figure 7B,C, the presence of NP decreases the ratio of dynamic/static intensity of the hard-segment bands relative to the soft. This observation indicates that in the presence of NP the soft segments orient more with the dynamic strain than do the hard segments, opposite to what is observed for pure Estane. The orientation functions indicate that the presence of NP significantly diminishes both hard- and soft-segment orientations. Near 600% strain, both segments still possess linear responses with no indication of orientation saturation. With increasing NP (Table 2), the ratios of the hard-segment bands (dynamic/static) tend to decrease significantly, while those of the soft-segment bands stay relatively close to 1.

For many of the bands, the maxima in the in-phase dynamic spectra are shifted with respect to those in the corresponding static spectrum. These spectral features are similar in shape to the bipolar bands which arise from frequency shifts in the stretched versus relaxed state of the polymer. This type of behavior has been frequently observed in dynamic dichroic spectra.[9,13,33,34] However, the bands of Estane and plasticized Estane in the current data are not definitively bipolar and arise from frequency shifts coupled with significant intensity changes.[34] The result is a slightly bipolar band, shifted rather than being fully derivative-shaped. The most pronounced shifts originate from soft-segment bands in the samples containing NP, with several hard-segment bands showing this behavior as well. The only bands that do not show this trait are those at 1730, 1360, 1394, and 1415 cm^{-1}. The dynamic dichroic band maxima tend to occur at lower frequencies compared to the corresponding static dichroic spectra.

Kischel et al.[13] have attributed the appearance of specific bimodal bands in dynamic dichroic spectra of an elastomer to hydrogen-bonding pairs in the polymer. This interpretation may account for some of the observed shifts in the current data, but bands not involved in hydrogen bonding show frequency shifts as well. These changes must be attributed to stress-induced polymer deformation, with bimodal bands arising from frequency shifts between the parallel and perpendicular components of a band.

The dynamic frequency shifts of the Estane bands are larger in the presence of NP. Assuming that the majority of NP molecules are solubilized in the soft domain, the polymer network established by the pseudo-crosslinks of the aligned hard segments may then be more highly constrained to the forces of unidirectional alignment. Upon static stretching, the distorted network has time to "relax" back to a relatively low orientation state with less bond distortion. In contrast, when a preoriented sample is deformed dynamically, components rapidly pulled parallel or perpendicular are distinguished. The parallel (positive) components are the dominant contributors to the spectrum in each case (Figure 6), since the majority of vibrational dipoles are aligned in the strain direction.

Conclusions

FT-IR static and dynamic linear dichroism studies provide a means of exploring polymeric deformations caused by unidirectional stretching and also the molecular-level effects of plasticization.

In pure Estane, the results indicate that, with static stretching on a 15 min time scale, the soft domains reach an orientation saturation earlier than the hard domains.[11] Several soft domain bands are highly sensitive to the degree of static stretch. With added NP, hydrogen bonding to the hard segments is disrupted and the glass transition of the soft domain decreases, indicating that a significant amount of the NP remains solubilized in the soft domains. The effect of NP on the static stretching is to diminish the ability of both elastomeric domains to orient (or to remain oriented 15 min after the increase in strain). NP itself does not orient significantly. The frequency shifts in the soft domains of NP-containing samples are diminished and delayed, taking place only at higher static strains. In the presence of NP, neither domain is orientationally saturated during the prestretching process, and the dynamic distortion results in a similar response from both domains. Bimodal bands in the dynamic data indicate that the strain applied on a rapid time scale (20 Hz) allows resolution of the components of differently oriented bands. In addition, the presence of NP increases the magnitude of these bimodal frequency shifts.

The present work demonstrates a unique advantage in using dichroic difference spectroscopy to study the effect of plasticization on polymers. In FT-IR spectra, NP bands dominate and mask many of the polymer bands, whereas in dichroic difference FT-IR, the random NP dipoles do not contribute to the spectra, and the effect on the polymer bands can be more directly observed. Future work will use dichroic FT-IR to examine the molecular-level effects of aging on the polymer−NP composite and will incorporate measurements at or near the T_g of the soft domains.

Acknowledgment. The authors (J.R.S. and D.K.G.) acknowledge the Technical Partnership Program at LANL for support in this work. D.K.G. also thanks the LANL Director's Funded Postdoctoral Program for financial support. R.A.P. and H.W. acknowledge the support of the Lord Foundation of North Carolina, Bruker Optics, and Duke University. In addition, the PEM device used in this study was graciously loaned to us by Hinds Instruments.

References and Notes

(1) Fawcett, A. H. E. *Polymer Spectroscopy*; John Wiley & Sons Ltd.: Chichester, 1996.
(2) Koenig, J. L. *Spectroscopy of Polymers*; American Chemical Society: Washington, DC, 1992.
(3) Estes G. M.; Seymour R. W.; Cooper, S. L. *Macromolecules* **1971**, *4*, 452.
(4) Siesler H. W.; Perl, W. *Mikrochim. Acta* **1988**, *I*, 323.
(5) Siesler H. W. *Polym. Bull.* **1983**, *9*, 382.
(6) Siesler H. W. *Ber. Busenges. Phys. Chem.* **1988**, *92*, 641.
(7) Siesler H. W. *Makromol. Chem., Makromol. Symp.* **1992**, *53*, 89.
(8) Sonoyama, M.; Shoda, K.; Katagiri, G.; Ishida, H. *Appl. Spectrosc.* **1996**, *50*, 381.

(9) Budevska, B. O.; Manning, C. J.; Griffiths, P. R.; Roginski, R. T. *Appl. Spectrosc.* **1993**, *47*, 1843.
(10) Gregoriou, V. G.; Chao, J. L.; Toriumi, H.; Palmer, R. A. *Chem. Phys. Lett.* **1991**, *179*, 491.
(11) Wang, H. W.; Graff, D. K.; Schoonover, J. R.; Palmer, R. A. *Appl. Spectrosc.* **1999**, *53*, 687.
(12) Singhal, A.; Fina, L. J. *Appl. Spectrosc.* **1995**, *49*, 1073.
(13) Kischel, M.; Kisters, D.; Strohe, G.; Veeman, W. S. *Eur. Polym. J.* **1998**, *34*, 1571.
(14) Noda, I.; Dowrey, A. E.; Marcott, C. *J. Mol. Struct.* **1990**, *224*, 265.
(15) Pezolet, M.; Pellerin, C.; Prudhomme, R. E.; Buffetueau, T. *Vib. Spectrosc.* **1998**, *18*, 103.
(16) Hoffman, U.; Pfeiffer, F.; Okretic, S.; Volkl, N.; Zahedi, M.; Siesler, H. W. *Appl. Spectrosc.* **1993**, *47*, 1531.
(17) Hoffman, D. M.; Caley, L. E. Dynamic Mechanical and Molecular Weight Measurements on Polymer Bonded Explosives from Thermally Accelerated Aging Tests II. A Poly(ester-urethane) Binder, Lawrence Livermore National Laboratory, 1981.
(18) Pegoretti, A.; Kolarik, J.; Penati, A. *Angew. Makromol. Chem.* **1994**, *220*, 49.
(19) Foltz, M. F. *Propellants, Explos. Pyrotech.* **1994**, *19*, 63.
(20) Christenson, C. P.; Harthcock, M. A.; Meadows, M. D.; Spell, H. L.; Howard, W. L.; Creswick, M. W.; Guerra, R. E.; Turner, R. B. *J. Polym. Sci., Part B: Polym. Phys.* **1986**, *24*, 1401.
(21) Orler, E. B.; Wrobleski, D. A.; Smith, M. E. Jr., unpublished results.
(22) Mishra, V.; Thomas, D. A.; Sperling, L. H. *J. Polym. Sci., Part B: Polym. Phys.* **1996**, *34*, 2105.
(23) Aklonis, J. J.; MacKnight, W. J. *Introduction to Polymer Viscoelasticity*; John Wiley & Sons: New York, 1983.
(24) Graff, D. K.; Wrobleski, D. A.; Marsh, A. L.; Kober, E. M.; Smith, M. E.; Schoonover, J. R. Polymeric Materials: Science and Engineering. *Proceedings of the 215th Meeting of the American Chemical Society, Dallas, TX, 1998*; American Chemical Society: Washington, DC, 1998.
(25) Srichatrapimuk, V. W.; Cooper, S. L. *J. Macromol. Sci., Phys.* **1978**, *15*, 267.
(26) Graff, D. K.; Clark, S.; Kreinbrink, K.; Kober E. M.; Schoonover, J. R., manuscript in preparation.
(27) Rodriguez-Cabello, J. C.; Merino J. C.; Pastor J. M.; Hoffmann, U.; Okretic, S.; Siesler, H. W. *Macromol. Chem. Phys.* **1995**, *196*, 815.
(28) Rodriguez-Cabello, J. C.; Merino, J. C.; Jawhari, T.; Pastor, J. M. *Polymer* **1995**, *36*, 4233.
(29) Rodriguez-Cabello, J. C.; Merino, J. C.; Jawhari, T.; Pastor, J. M. *J. Raman Spectrosc.* **1996**, *27*, 463.
(30) Wool, R. P.; Bretzlaff R. S.; Li B. Y.; Wang C. H.; Boyed, R. H. *J. Polym. Sci., Part B: Polym. Phys.* **1984**, *24*, 1039.
(31) Wool, R. P.; Boyd, R. H. *J. Appl. Phys.* **1980**, *51*, 5116.
(32) Hutchinson, I. J.; Ward, I. M.; Willis, H. A.; Zichy, V. *Polymer* **1980**, *21*, 55.
(33) Lagaron, J. M.; Steeman P. A.; Kip, B. J. *Appl. Spectrosc.* **1998**, *52*, 702.
(34) Ingemey, R. A.; Strohe, G.; Veeman, W. S. *Appl. Spectrosc.* **1996**, *50*, 1360.

MA990495G